UAS Pointclouds vs. Lidar Pointclouds for structual analysis of forests

Marvin Ludwig, Simon Seyfried, Chris Reudenbach, Thomas Nauss

Introduction

Use of LiDAR in nature conservation and forestry

Light detection and ranging (LiDAR) remote sensing is a well established tool in the assessment of biodiversity and nature conservation. From the raw 3D pointclouds, a large variety of information can be derived helping to explain and manage critical environmental processes like shrub encroachment in grasslands (Madsen et al. 2020), forest health assessment (Duncanson and Dubayah 2018) or the monitoring of wetland loss (Montgomery et al. 2019). One of the most common applications of LiDAR data is the description of the structure of landscapes, which then serve as drivers for species occurrence (Carrasco et al. 2019; Melin et al. 2016; Froidevaux et al. 2016) or as indicators for biodiversity (Hilmers et al. 2018; Simonson, Allen, and Coomes 2014).

Especially forest environments are a very popular target for analysis with LiDAR data (Beland et al. 2019). Structural information can be derived at the level of individual tree groups (Jeronimo et al. 2018) or individual crowns in sparse forest stands (Silva et al. 2016). However a more operational and well established approach is, to transfer the structural information of the 3D pointcloud into a regular 2D grid, commonly referred to as LiDAR indices. The vegetation structure then is represented e.g. as the vertical distribution or the maximum height of points in one grid cell (Bakx et al. 2019). In order to preserve some of the original 3D information, there are indices which work on voxel (i.e. horizontal slices of the pointcloud) and can represent different strata of the forest canopy (e.g. Alexander et al. 2014). The reliability of LiDAR indices is usually shown by referring them to field measurements of established forest structural indices like canopy cover and canopy height (J. Lee et al. 2018; Alexander et al. 2014), stand density (C.-C. Lee and Wang 2018) or leaf area (Kamoske et al. 2019).

Problems with LiDAR

Despite their relevance in conservation and research, LiDAR data has some major drawbacks, mainly in their cost and accessibility. Professional LiDAR sensors are expensive and data acquisition are expensive and often distributed commercially. Data provided by governmental institutions are still irregularly available and often not publicly distributed. Further, the temporal resolution of the data is low (by law every 3 years in Germany) making them not suitable for monitoring or applications which require different seasonal conditions. Researchers also have no control over the acquisition time, however the environmental condition (e.g. leaf-on or leaf-off) has a direct impact on the derived LiDAR indices and therefore the product quality (Davison, Donoghue, and Galiatsatos 2020). It can also be beneficial to combine leaf off and leaf on LiDAR data, e.g. for improving the model quality of tree species classifications (Shi et al. 2018).

- some words and publications about LiDAR UAS

Use of UAS digital aerial photogrammetry

With the recent development of Unmanned Aerial Systems (UAS) and improvements of photogrammetric image processing, an alternative to LiDAR pointclouds is available. Quick data access in moderately large areas makes UAS data promising for the monitoring of agricultural or natural systems (Manfreda et al. 2018). Depending on flight conditions, these pointclouds could be acquired on a near daily basis. Especially in forest environments, research can benefit from vegetation structural information retrieved from UAS data.

mix of pointclouds and images to classify individual trees (Xu et al. 2020) Tree height works good in UAS (Fawcett et al. 2019)

However, if trees are detected, the height measurement is well established and consistent across multiple flight dates (e.g. Krause et al. 2019)

Monitoring of Canopy height of crops with multitemporal UAS based CHMs, DEM was build manually with known ground point interpolation (Grüner, Astor, and Wachendorf 2019)

also comparing well to TLS based pointclouds when evaluating plant height in agriculture (Malambo et al. 2018)

Previous comparisons of UAS and Lidar

comparison of lidar and uav CHM (Michez et al. 2020)

Comparison of Lidar and UAS based pointclouds for individual tree height (Ganz, Käber, and Adler 2019) revealed very good compariability. Quality of UAS based studies is highly depended on the accuracy of data acuisition and ulitmately proper georeferencing. Dealed with that in Ludwig 2020!

Comparisons revealed good potential of UAS pointclouds as a substitude for lidar when estimating common forest attributes (e.g. Ullah et al. 2019; Cao et al. 2019) and to a lesser extent biomass estimations in the tropics (Ota et al. 2015)

DEM clearly is the week point of photogrammetry (Ota et al. 2015) When comparing ALS and UAS, using a ALS derived DTM is common in order to normalize the Pointclouds (e.g. Ullah et al. 2019)

UAS pointclouds do not have return values which many Lidar indices depend on. Every point is a first return so we cannot get below a developed canopy. These return values however are crucial for LiDAR point classification (e.g. differentiate between ground and non ground point).

EBV framework with 3D information: height, cover and structural complexity Heterogenous data sources: requires the comparability of Lidar and photogrammetrically recieved pointclouds (Valbuena et al. 2020)

The quality and viability of UAS pointclouds have to be assessed in terms of comparability to Lidar pointclouds (since Lidar structural analysis is the standard in many studies)

Previous work of multitemporal UAS

Multitemporal UAV for monitoring coral reefs (Fallati et al. 2020)

Multitemporal UAS can benefit monitoring, e.g. tree growth rates (Guerra-Hernández et al. 2017) or crops (Moeckel et al. 2018)

Multitemporal UAS orthoimages can enhance classification of vegetation types slightly (van Iersel et al. 2018), makes use of plant phenology, most imprtant were july and september because there, green vegetation were at the maximum

Biomass of single trees (in a park) much better under leaf off conditions (Ye, van Leeuwen, and Nyktas 2019)

If the positional accuracy of the individual photogrammetric pointclouds is high enough (previously shown in Ludwig et al. (2020), it is a resonable assumption to combine pointclouds from different phenological stages in order to get a full 3D model of the forest.

Since photogrammetically received pointclouds only capture the surface and do not penetrate the forest canopy like Lidar pointclouds, different phenological stages should capture different vertical layers of the forest canopy.

What we do

Since most LiDAR indices are are strongly correlated (Shi et al. 2018) we picked 4 commonly used indices from (Bakx et al. 2019)

This study demonstates the usability of multitemporal pointclouds derived from digital aerial photogrammetry for forest structural analysis. Commonly applied forest structural indicators will be compared between DAP and LiDAR pointclouds for different spatial scales and different phenological stages of a deciduous forest. In addition we propose the combination of multiple DAP pointclouds as a way to improve their information value and better comparability to LiDAR data. All derived pointcloud indicators will also be related to commonly used forest structural indicators from field surveys of trees.

Hypothesis 1: When compared to LiDAR pointclouds, the quality of structural indices from DAP pointclouds depend on the phenological stages of a deciduous forest.

Hypothesis 2: Multitemporal DAP pointclouds are superior than monotemporal pointclouds and are suitable to complement LiDAR derived pointclouds for forest structural analysis.

Methods

Study Area

As the study area serves a 200 x 200 m part of a mixed deciduous forest near Marburg (Germany). The area consists of oaks (*Quercus spec.*) and beeches (*Fagus sylvatica*) and represent a typical stand in a managed deciduous forest. Terrain elevation ranges from 250 m to 275 m a.s.l. Stem positions of 500 trees were acquired by using a differential GPS (Zenith 35 Pro, GeoMax Widnau Switzerland) with a positioning accuracy of 0.05 m.\

Datasets

The LiDAR data was acquired with a Riegl LMS-Q780 sensor in early spring 2018 under leaf off conditions (Tab. @ref(tab:tabDatasetOverview)) and provided by the Hessian Agency for Nature Conservation, Environment and Geology - HLNUG. The original pointcloud had an average point density of XX points per square meter with a georeferencing accuracy of 0.3 m horizontally and 0.15 m vertically (Novatel OEM4 GNSS). The LiDAR pointcloud was already classified into ground points and non-ground points by the data provider.
The DAP pointclouds were acquired with a 3DR Solo Quadrocopter (3D Robotics, Inc., Berkeley CA, USA) and a GoPro Hero 7 camera (GoPro Inc., San Mateo CA, USA) between August and December of 2020. The flight tasks were planned in a uniform altitude above ground at 110 m resulting in a ground sampling distance of 5.6 cm, a side overlap of 75% and a front overlap of 90%. Using the photogrammetric software Metashape (Agisoft LLC, St. Petersburg, Russia), sparse pointclouds were computed from the individual images of each flight. Each sparseclouds was georeferenced with 10 ground control points surveyed with the Real Time Kinematic (RTK) GNSS (Global Navigation Satellite System) device Geomax Zenith 35 (GeoMax AG, Widnau, Switzerland). A detailed explanation of the applied photogrammetic workflow is describe in (Ludwig et al. 2020). After the referencing, dense pointclouds were computed for each flight from non-resampled depth maps and moderate filtering.

ID	Type	Sensor	Acquisition Date Y-M-D	Description
1	LiDAR	Riegel LMS-Q780	2018-04-06	leaf off
2	DAP	GoPro Hero7	2020-09-15	full canopy
3	DAP	GoPro Hero7	2020-10-28	full canopy / beginning of coloring
4	DAP	GoPro Hero7	2020-10-31	early leaf fall
5	DAP	GoPro Hero7	2020-11-03	advanced leaf fall
6	DAP	GoPro Hero7	2020-11-12	advanced leaf fall
7	DAP	GoPro Hero7	2020-12-10	leaf off

Pointcloud preprocessing and combination

In order to increase the comparability between the pointclouds, each one was homogenized to a density of 50 points per square meter. The classified LiDAR ground points were used to compute a digital elevation model (DEM) with a spatial resolution of 1 m using a k-nearest neighbor algorithm with inverse distance weighting. The DEM was used to normalize the height of each pointcloud which effectively results in a canopy height model (CHM). To eliminate the effects of ground points in the upcoming index calculation, points below 2 m canopy height were removed.

DAP pointclouds from five different phenological stages during fall 2020 were combined with the leaf-off DAP pointcloud from 2020-12-11. These five multitemporal pointclouds were preprocessed the same way as the individual pointclouds (Fig. @ref(fig:figWorkflow)). All pointcloud based methods and computations were done in R using the lidR package (Roussel et al. 2020).

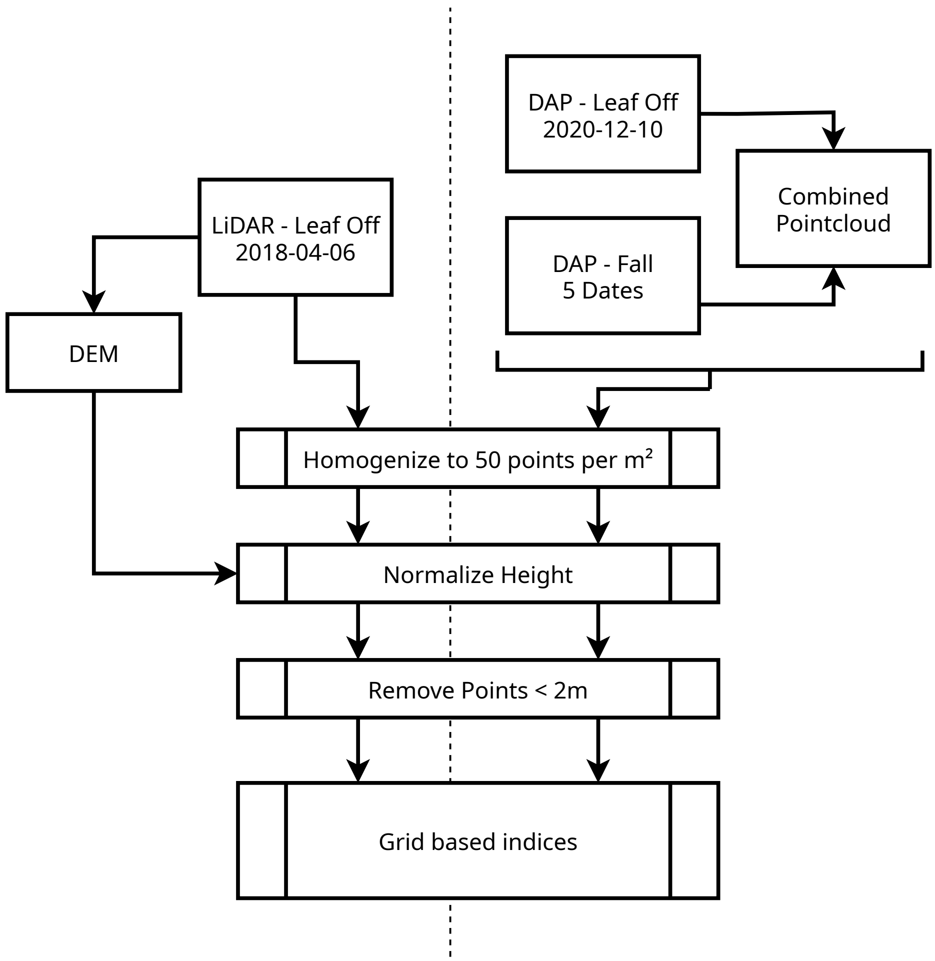

Common lidar indices

Canopy cover

Usually canopy cover is derived from LiDAR as follows (over 10 different studies cited in Bakx et al. (2019) Supplementary Material 3)

$$\frac{N_{p>x}}{N_t} * 100$$

with percentage of returns (Np > x) above x meter above ground level at the raster resolution. Nt is the total number of returns. Bakx et al. (2019) also mentiones Farrell et al. 2013 in which a tow part procedure is described: First cover is estimated from aerial photographs, then it is corrected by excluding areas with low canopy height derived from LiDAR. UAS based pointclouds might very suitable for this approach, since the pointcloud and the aerial image are received in the same workflow.

Canopy height

Maximum canopy height (z_max) Highest LiDAR return in a raster cell (over 10 different studies cited in Bakx et al. (2019) Supplementary Material 3)

$$Z_{max}$$

Mean canopy height 95% (z_mean95) Mean height of the returns in the 95 percentile (Z95). N95 is the number of returns in the 95 percentile

$$Z_{mean95} = \frac{\Sigma(Z_{95})}{N_{95}}$$

Mean canopy height (z_mean_csm) Mean height of the canopy surface model (CSM) in the grid cell (first return of the LiDAR). For Gap correction only points above a certain threshold are used (over 10 different studies cited in Bakx et al. (2019) Supplementary Material 3)

Horizontal canopy variability (index_name_sd)

Usually the standard deviation of the canopy cover or canopy height in larger raster cell (e.g. 10 m - reasonable to get to the sentinel scale!)

Vertical canopy variability

Coefficient of variation of canopy height (CV) Ratio between mean canopy height (Zmean) and standard deviation (Zsd) of canopy height (5 different studies cited in Bakx et al. (2019))

$$CV = \frac{Z_{mean}}{Z_{sd}}$$

Standard deviation of canopy height (z_sd_csm) Standard deviation of first returns in a raster cell (over 10 different studies cited in Bakx et al. (2019) Supplementary Material 3)

Results

Direct comparison of Lidar and DAP

Common Indices for different resolutions

Voxel mean height at different resolutions

Horizontal heterogenity

```
## [[1]]
```

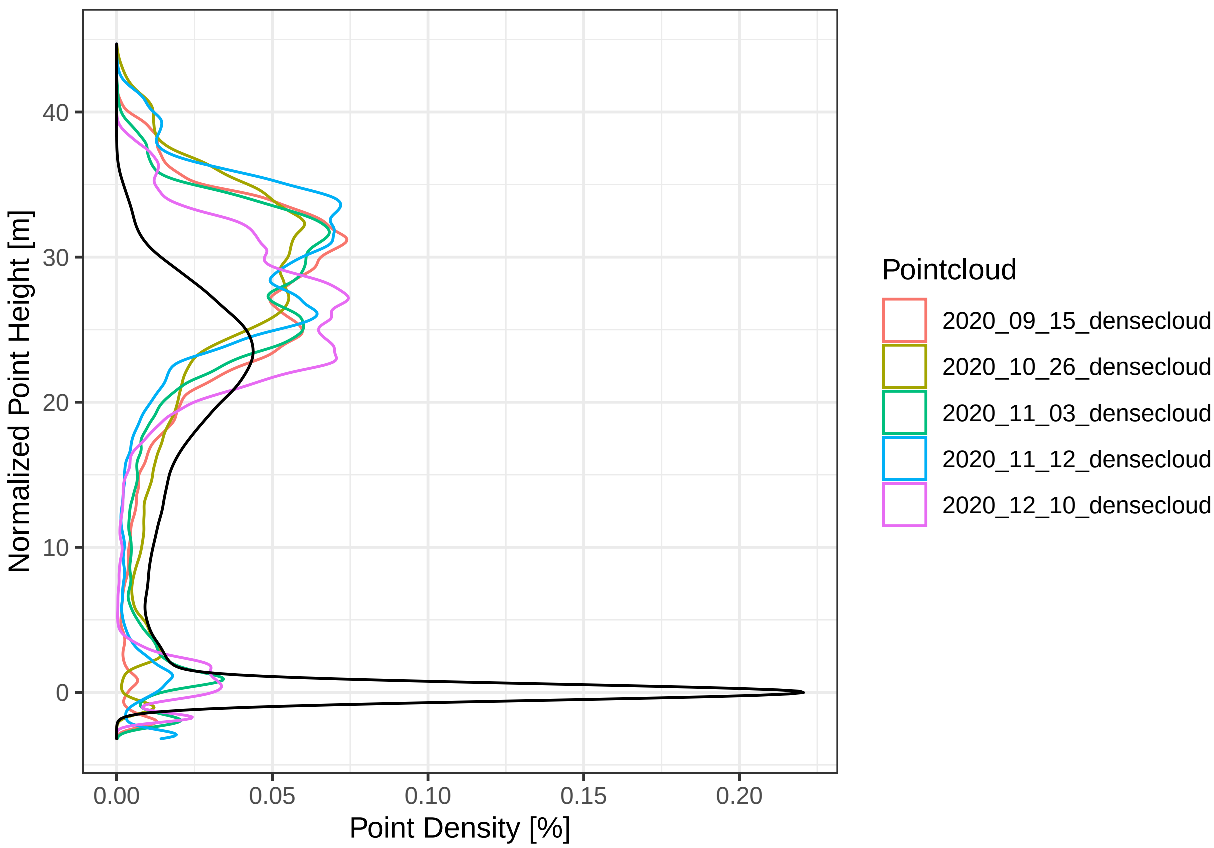

Figure 1: Comparison of the vertical point distribution of LiDAR and single date DAP

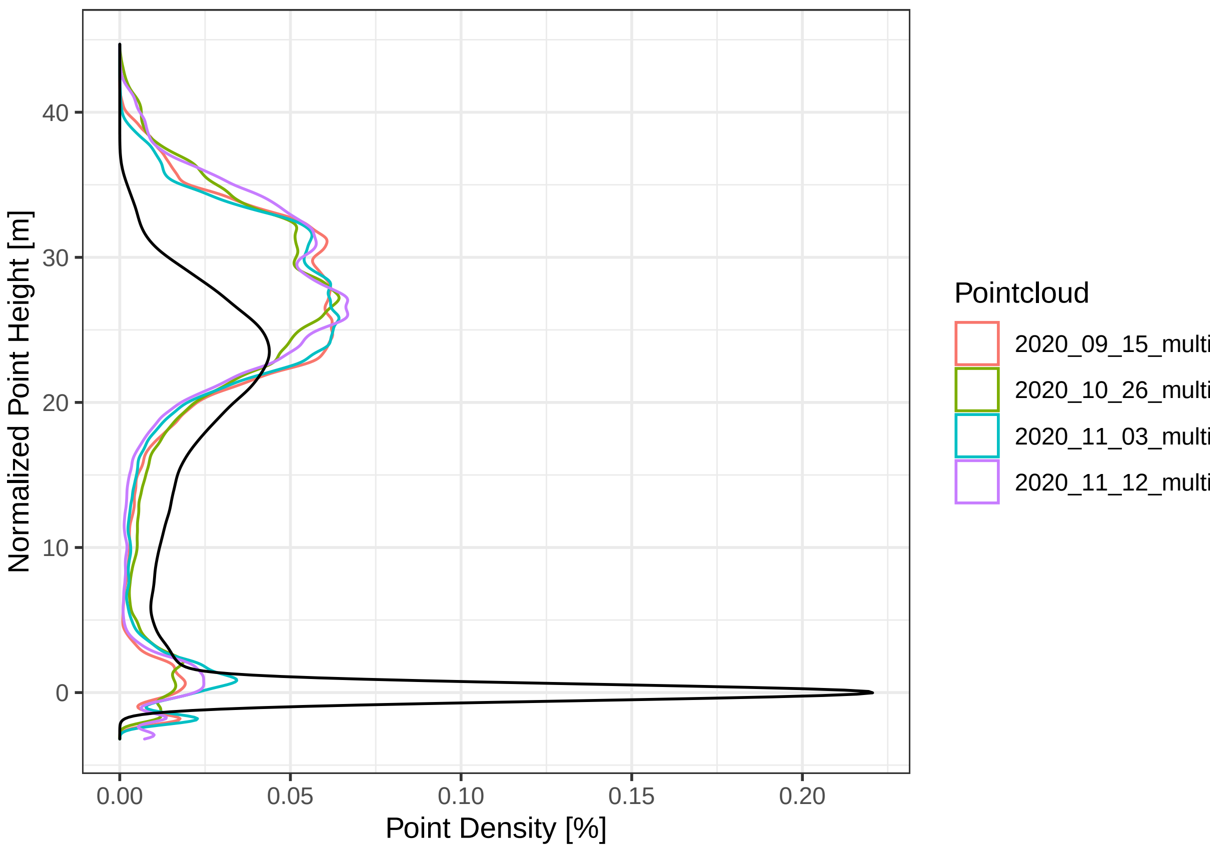

Figure 2: Comparison of the vertical point distribution of LiDAR and combined DAP in spring and fall

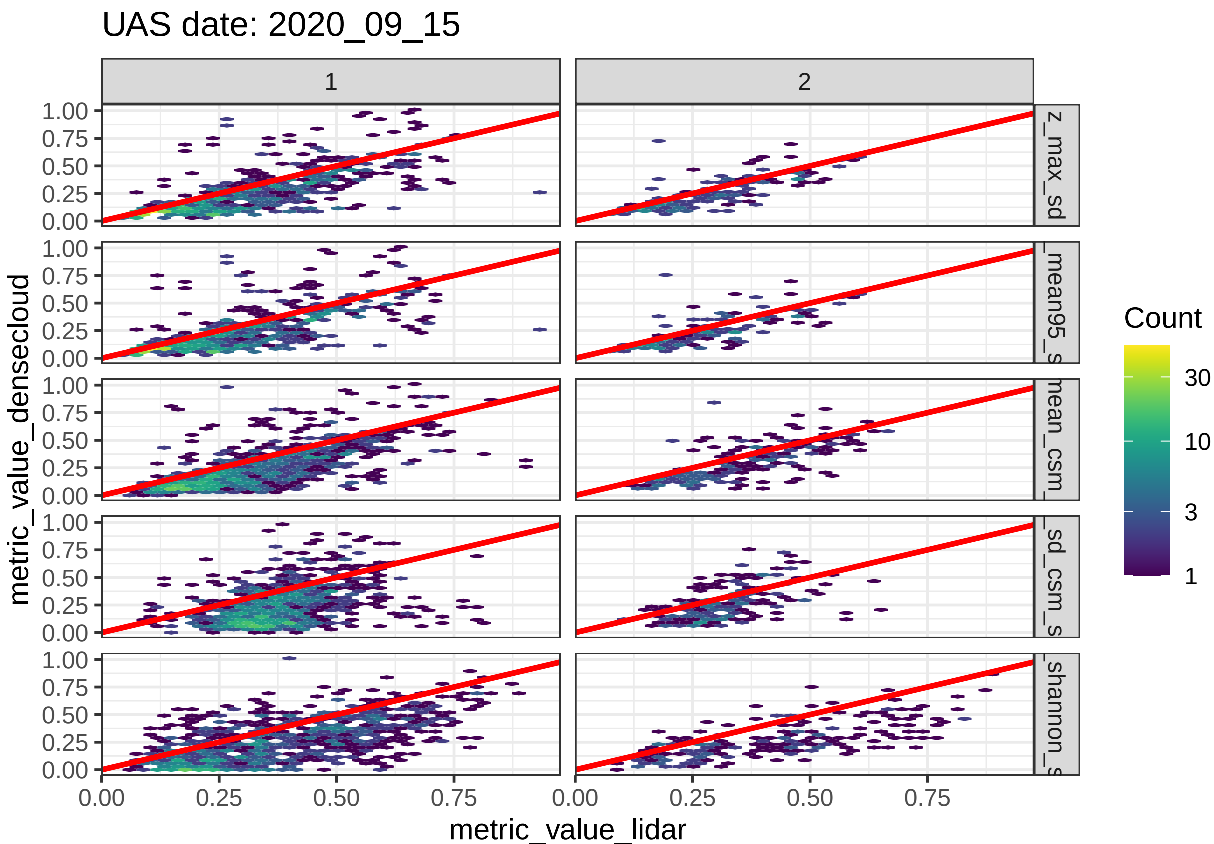
UAS date: 2020_09_15
1
2
z_max_sd
mean95_s
mean_csm
sd_csm_s
shannon_s
metric_value_densecloud
metric_value_lidar
0.00
0.25
0.50
0.75
1.00
Count
30
10
3
1

```
##
## [[2]]
```

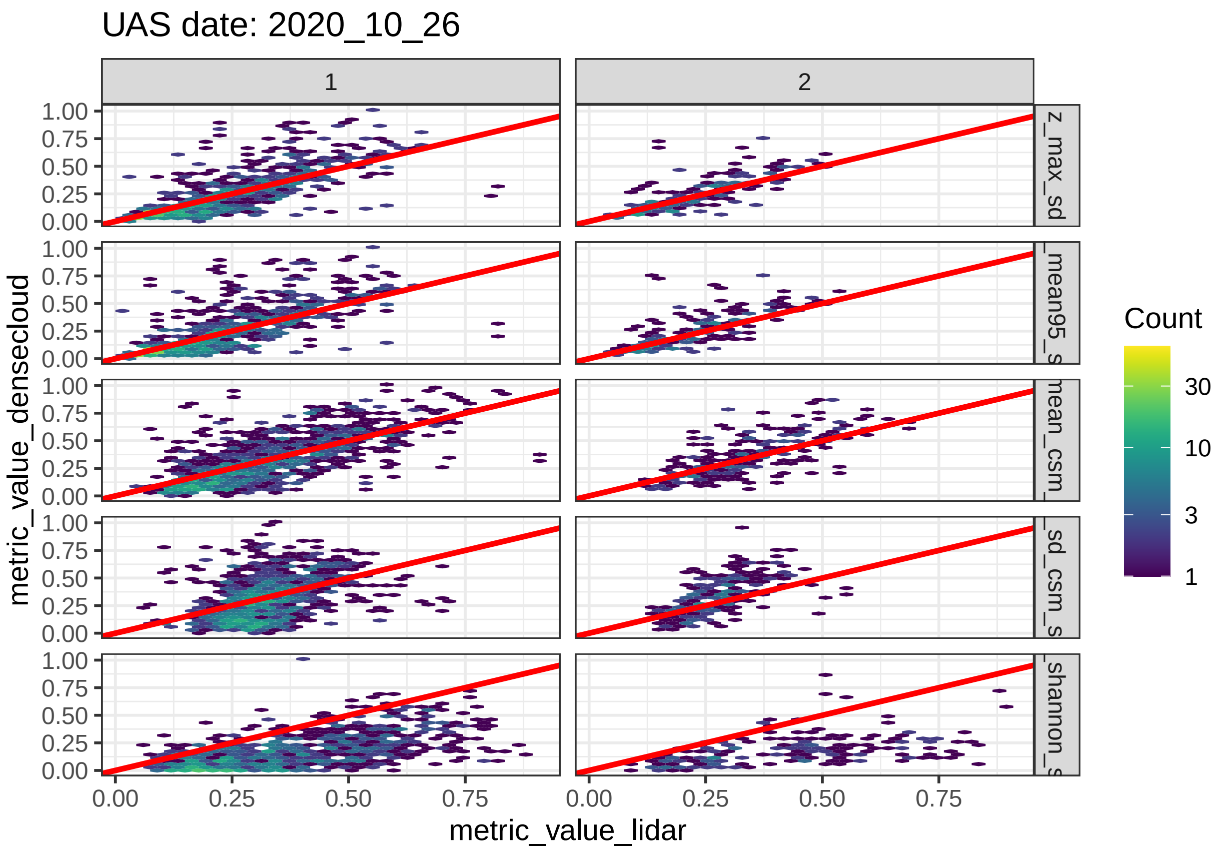
UAS date: 2020_10_26
1
2
z_max_sd
_mean95_s
mean_csm_
_sd_csm_s
shannon_s
metric_value_densecloud
metric_value_lidar
1.00
0.75
0.50
0.25
0.00
0.00
0.25
0.50
0.75
Count
30
10
3
1

```
##
## [[3]]
```

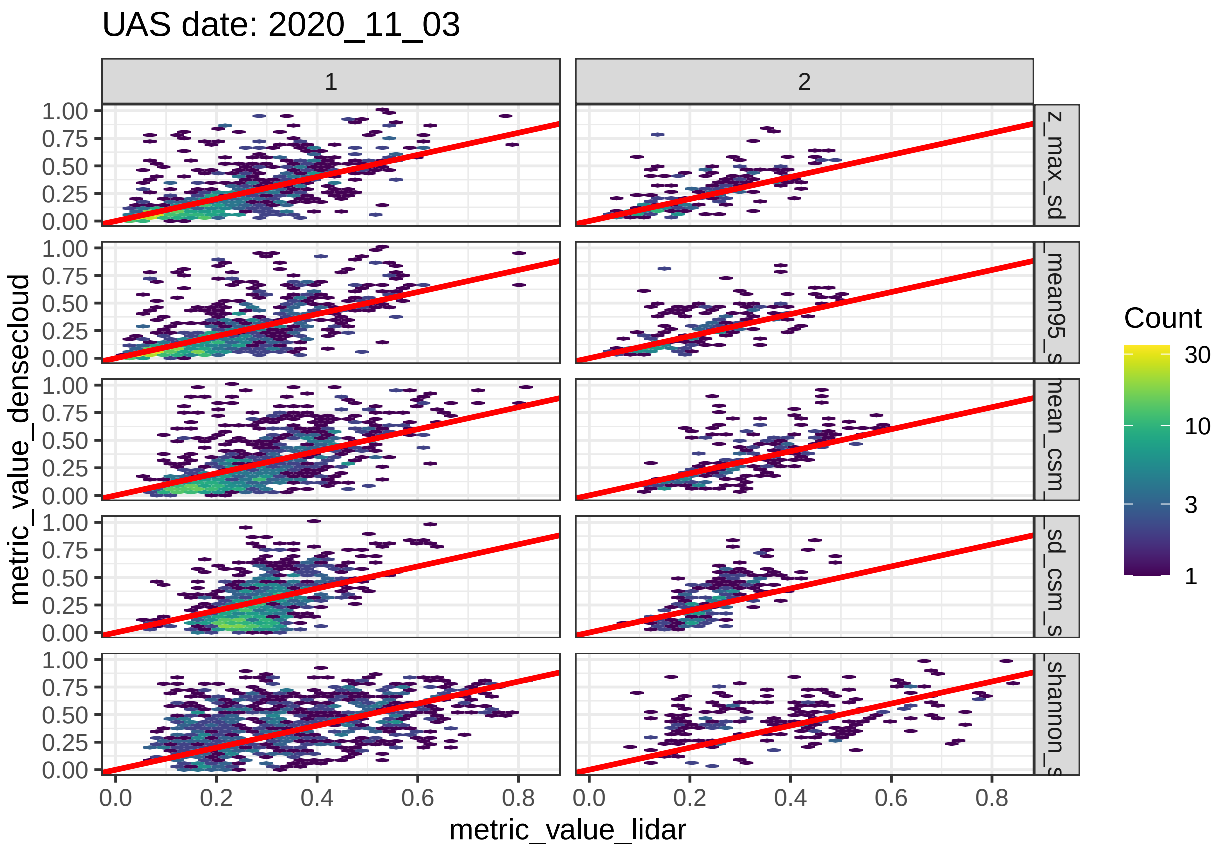

UAS date: 2020_11_03
1
2
z_max_sd
_mean95_s
mean_csm_
_sd_csm_s
shannon_s
metric_value_densecloud
metric_value_lidar
1.00
0.75
0.50
0.25
0.00
0.0
0.2
0.4
0.6
0.8
Count
30
10
3
1


```
##
## [[4]]
```

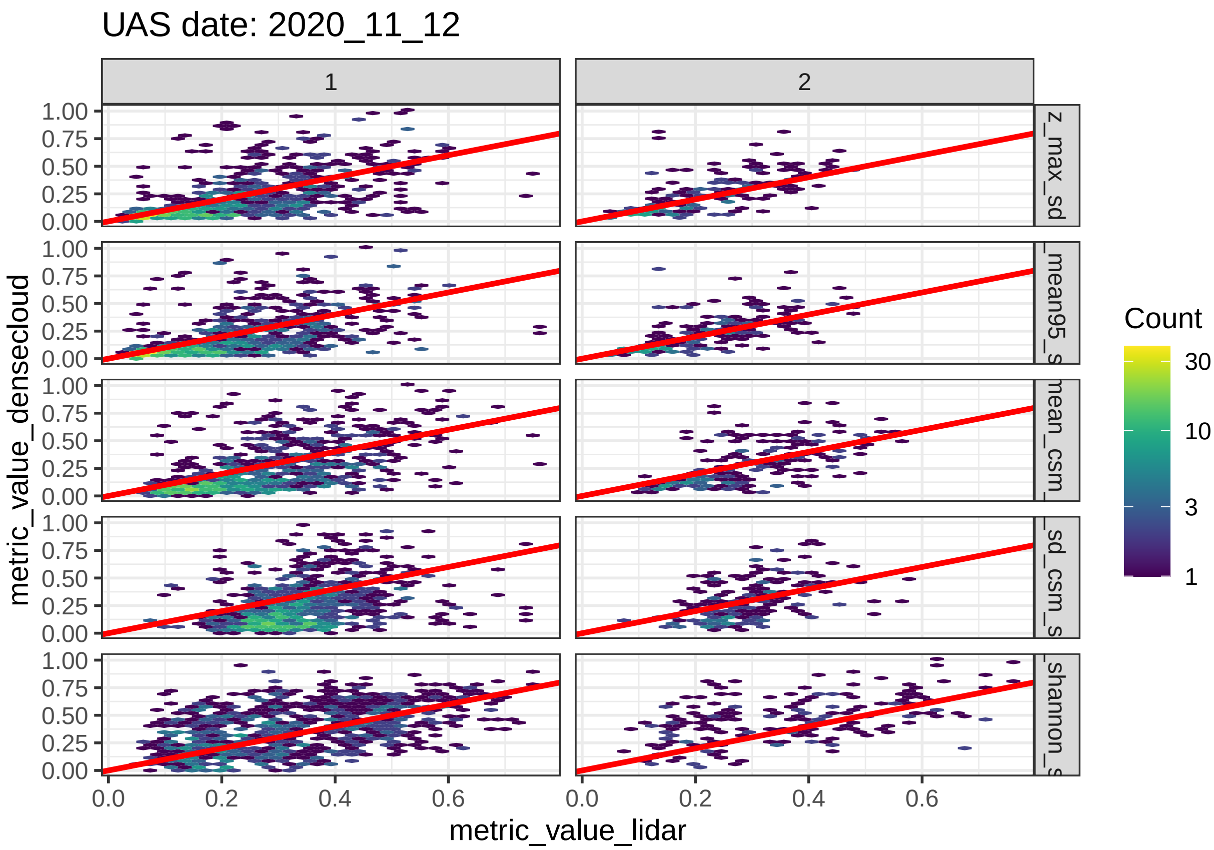

UAS date: 2020_11_12
1
2
z_max_sd
_mean95_s
mean_csm
_sd_csm_s
shannon_s
metric_value_densecloud
metric_value_lidar
1.00
0.75
0.50
0.25
0.00
0.0
0.2
0.4
0.6
Count
30
10
3
1


```
##
## [[5]]
```

UAS date: 2020_12_10

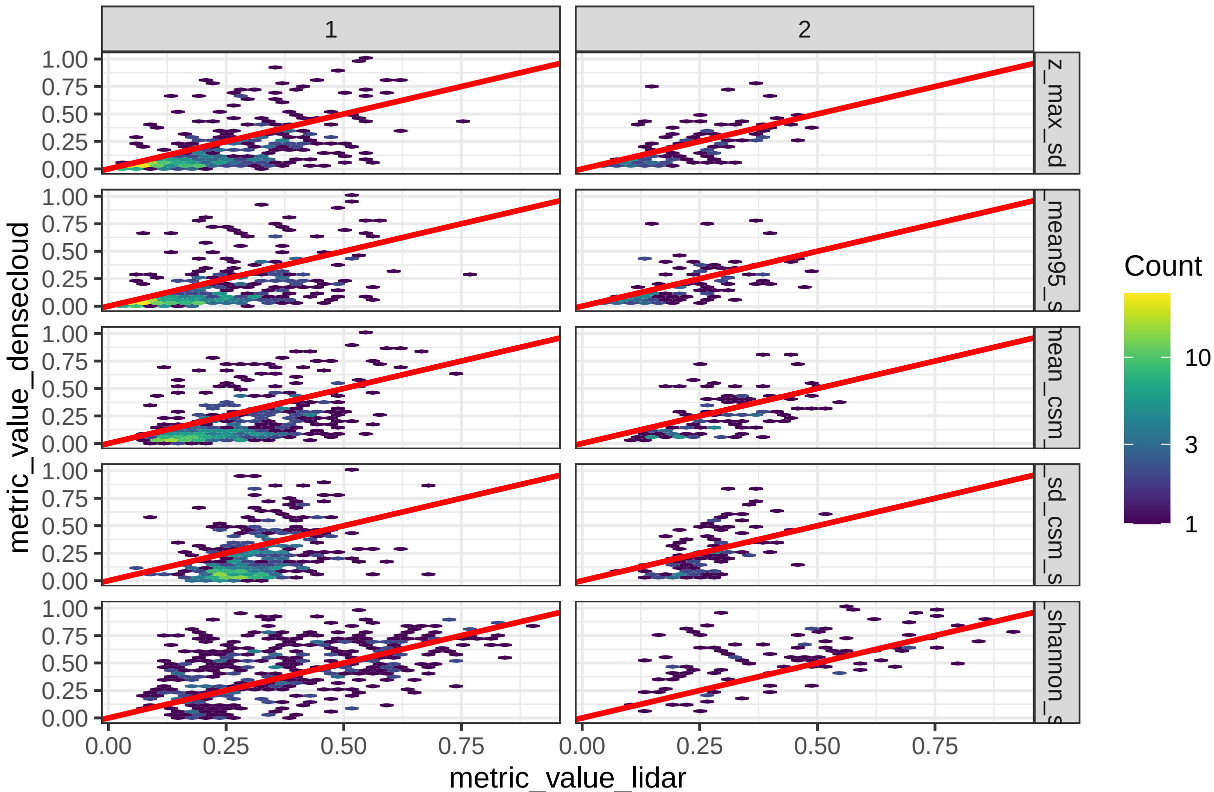

[[1]]

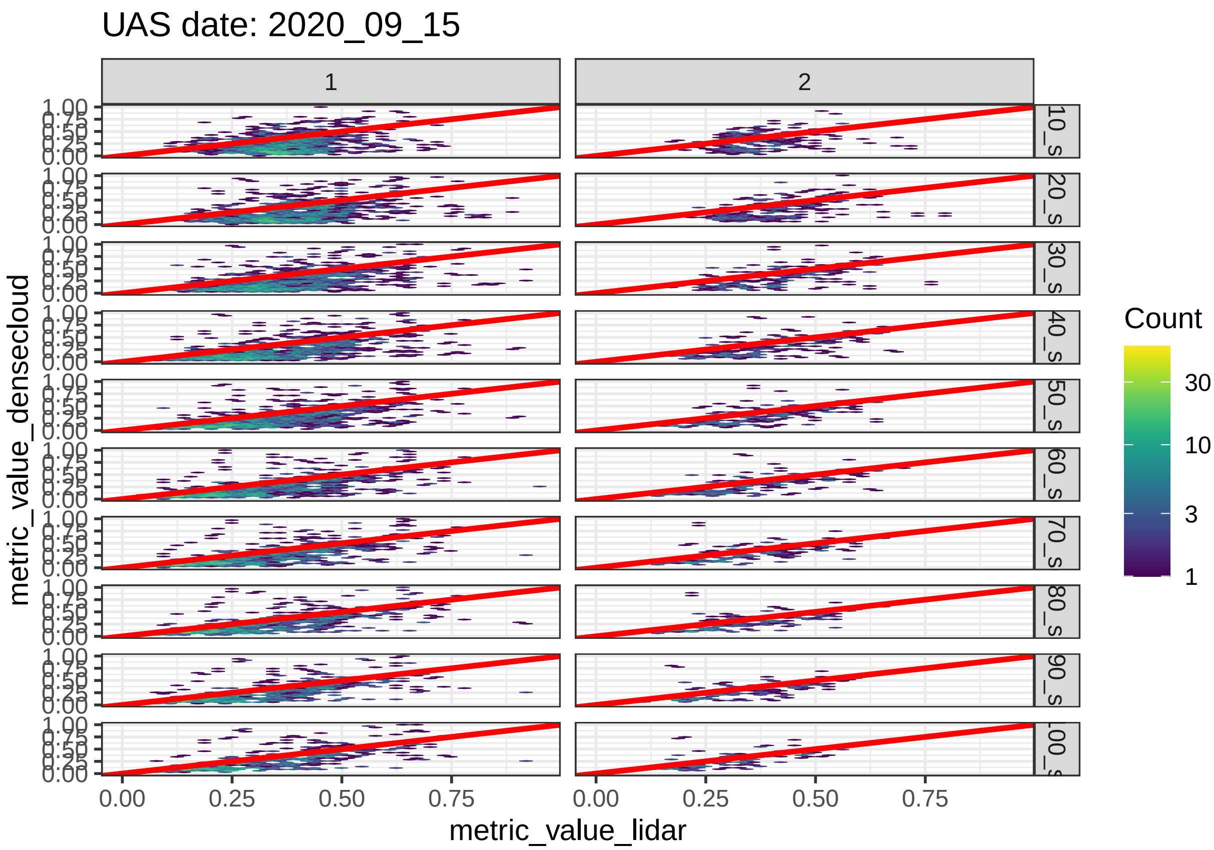

UAS date: 2020_09_15
1
2
10_s
20_s
30_s
40_s
50_s
60_s
70_s
80_s
90_s
100_s
metric_value_densecloud
metric_value_lidar
0.00
0.25
0.50
0.75
1.00
Count
30
10
3
1


```
##
## [[2]]
```

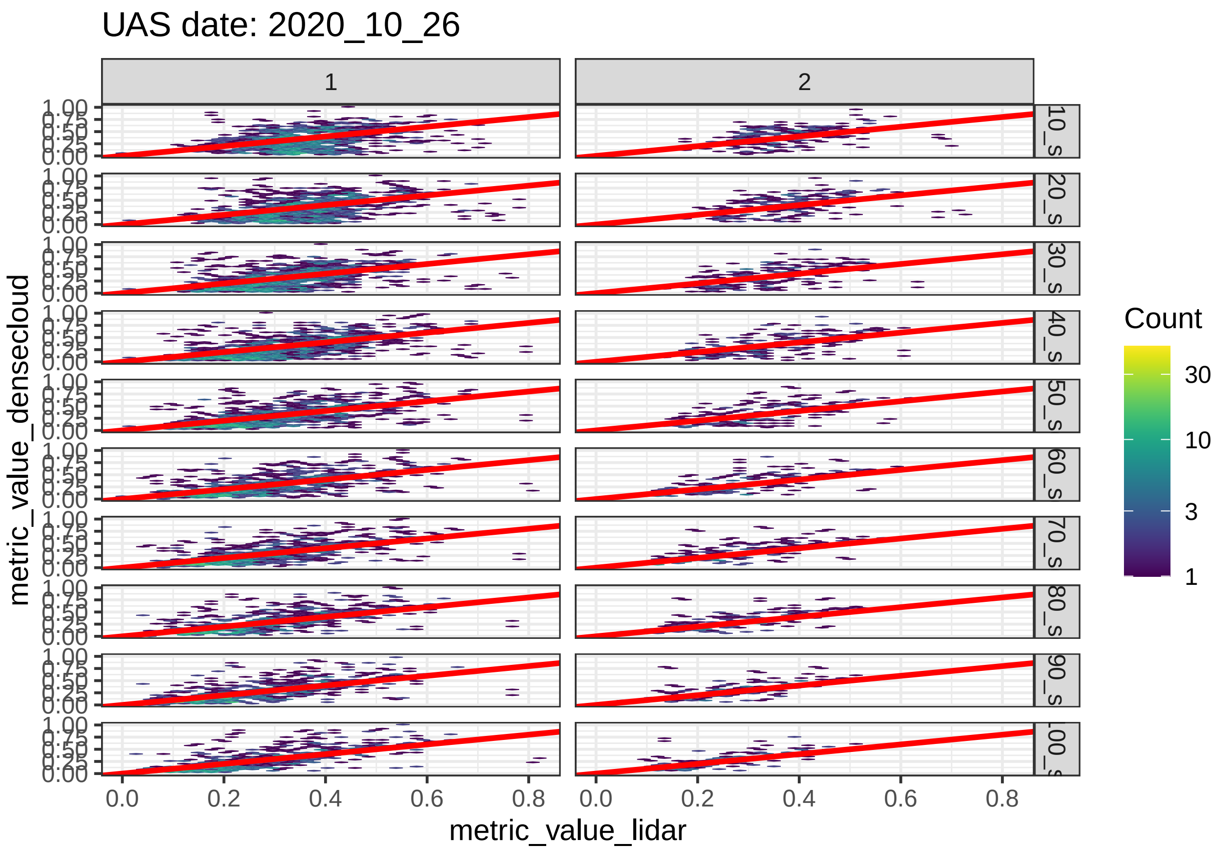
UAS date: 2020_10_26
1
2
10_s
20_s
30_s
40_s
50_s
60_s
70_s
80_s
90_s
metric_value_densecloud
metric_value_lidar
0.00
0.25
0.50
0.75
1.00
0.0
0.2
0.4
0.6
0.8
Count
30
10
3
1

```
##
## [[3]]
```

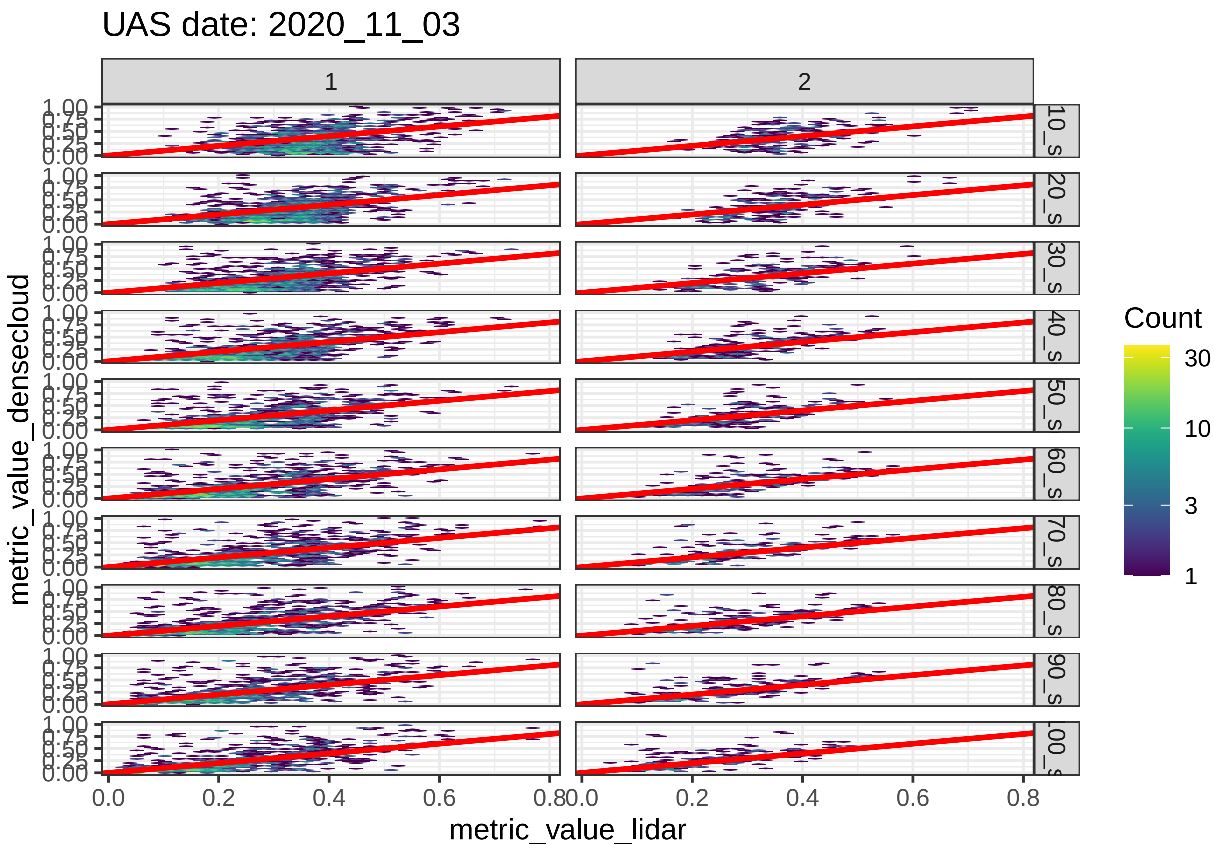
UAS date: 2020_11_03
1
2
10_s
20_s
30_s
40_s
50_s
60_s
70_s
80_s
90_s
metric_value_densecloud
0.00
0.25
0.50
0.75
1.00
metric_value_lidar
0.0
0.2
0.4
0.6
0.8
Count
30
10
3
1

```
##
## [[4]]
```

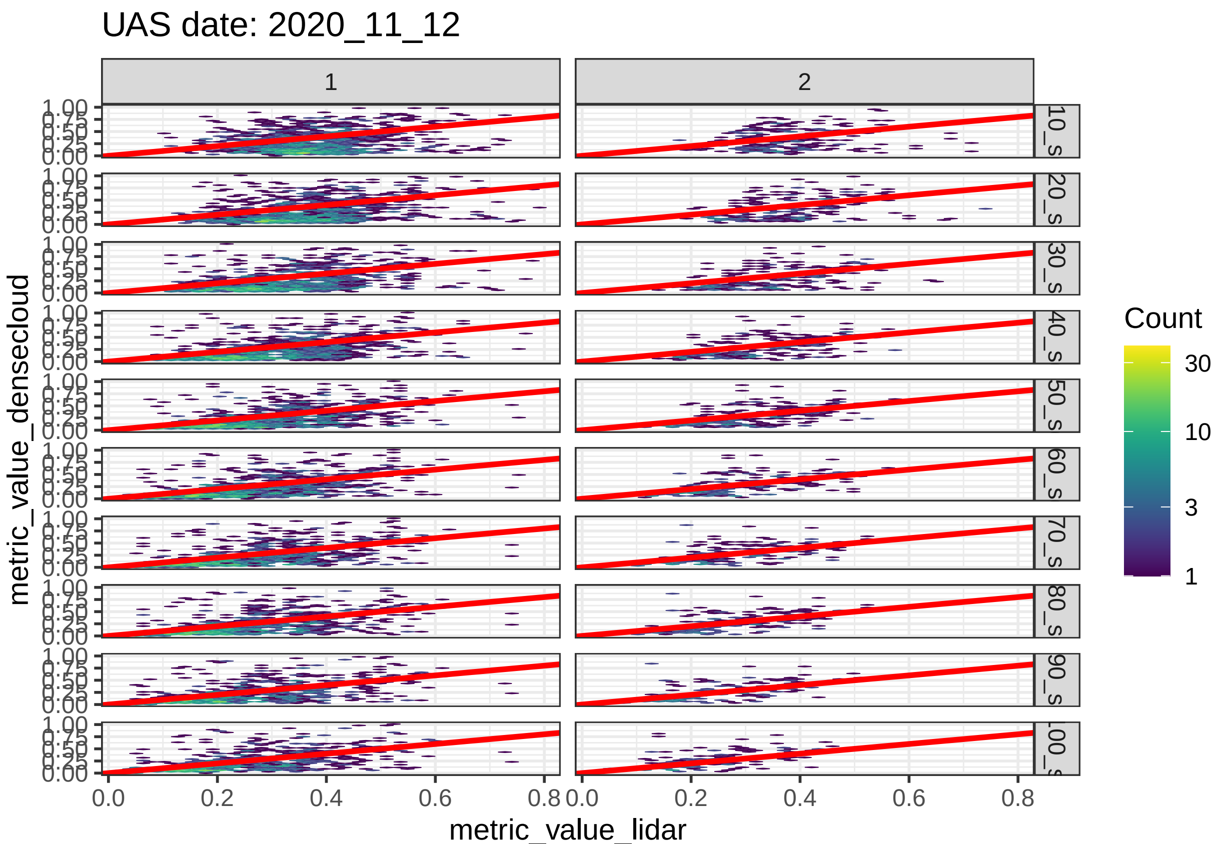
UAS date: 2020_11_12
1
2
10_s
20_s
30_s
40_s
50_s
60_s
70_s
80_s
90_s
100_s
metric_value_densecloud
metric_value_lidar
0.00
0.25
0.50
0.75
1.00
0.0
0.2
0.4
0.6
0.8
Count
30
10
3
1

```
##
## [[5]]
```

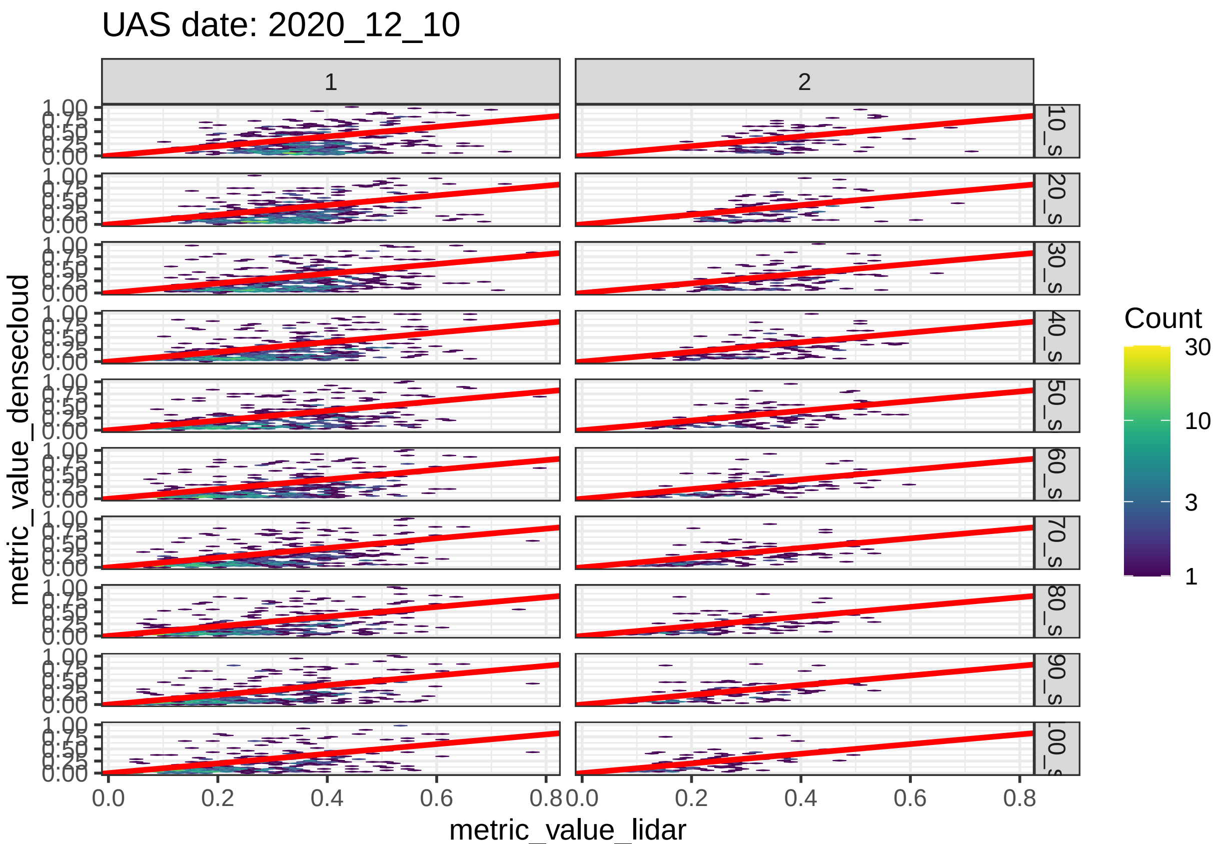

Multitemporal pointclouds

```
## [[1]]
```

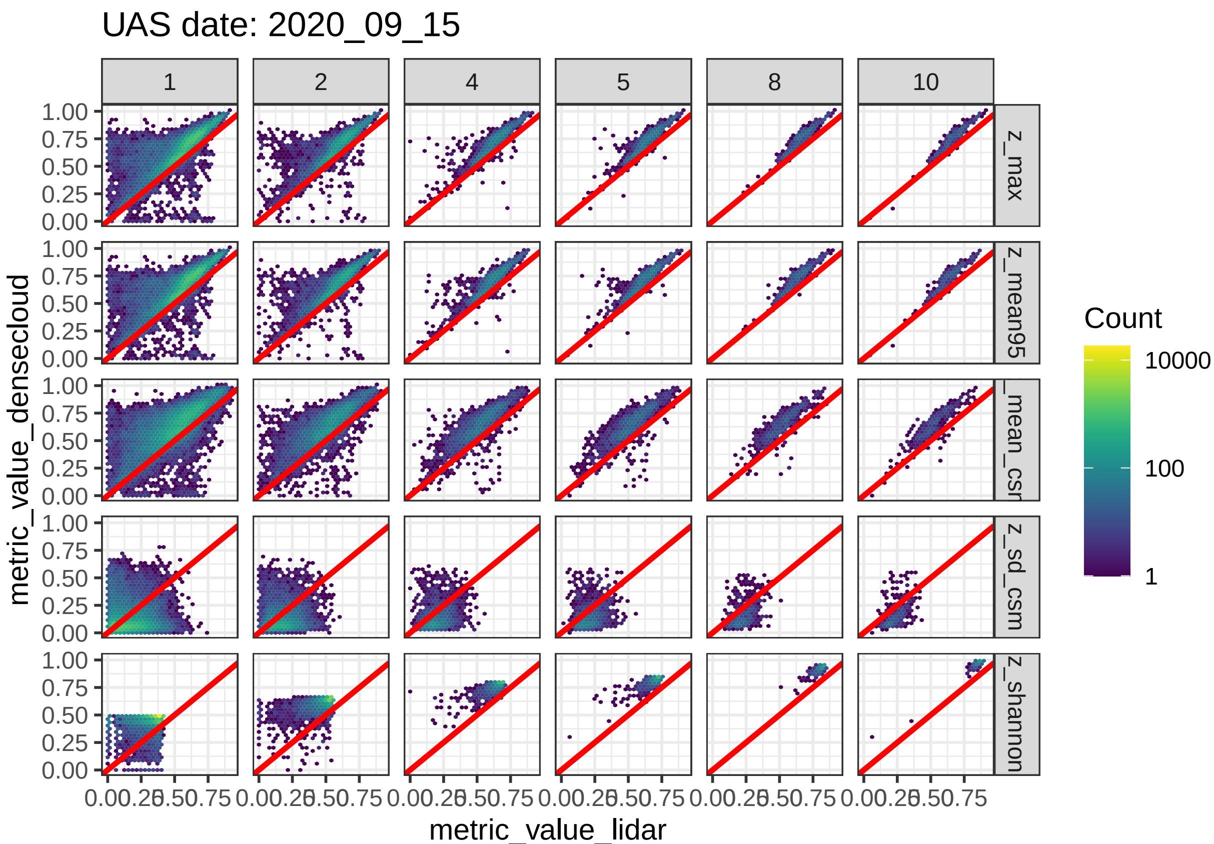
UAS date: 2020_09_15
1
2
4
5
8
10
z_max
z_mean95
_mean_csr
z_sd_csm
z_shannon
metric_value_densecloud
metric_value_lidar
1.00
0.75
0.50
0.25
0.00
0.00.250.50.75
Count
10000
100
1

```
##
## [[2]]
```

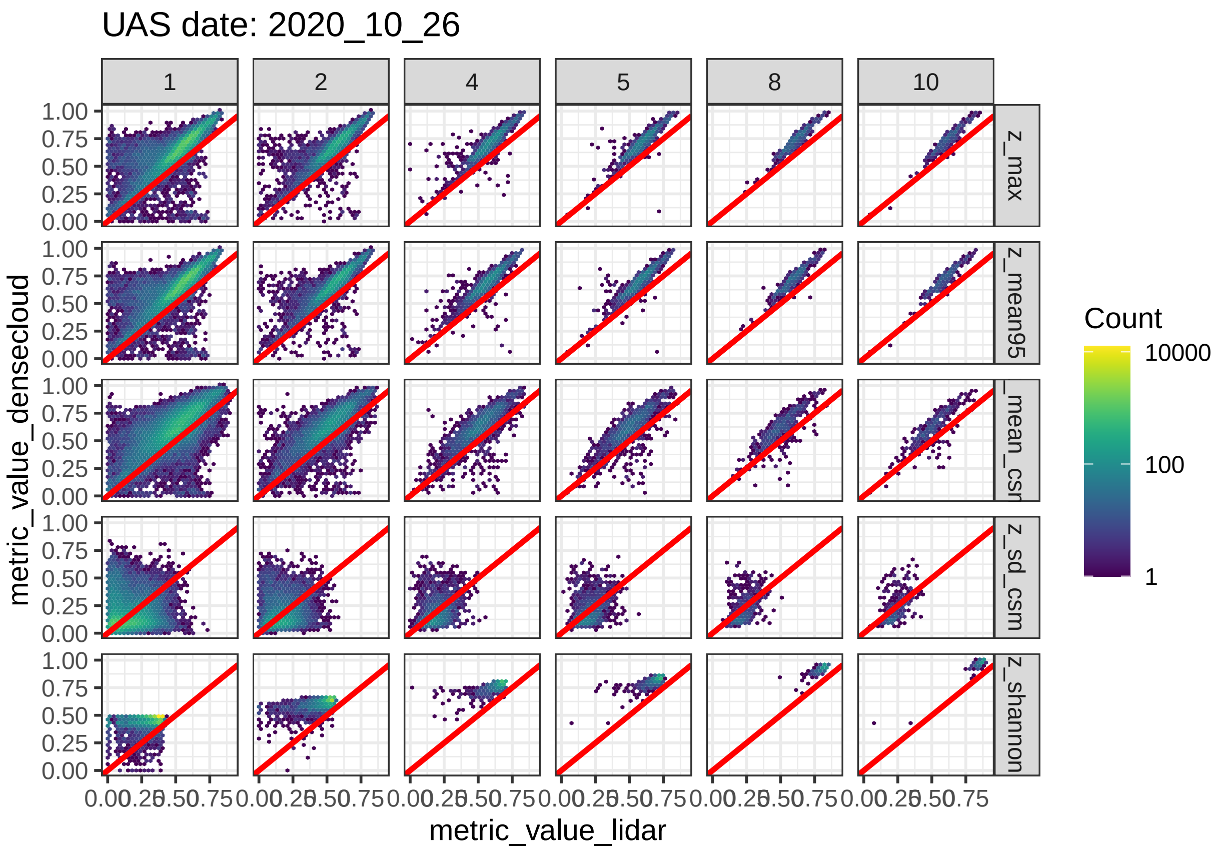
UAS date: 2020_10_26
1
2
4
5
8
10
z_max
z_mean95
_mean_csr
z_sd_csm
z_shannon
metric_value_densecloud
metric_value_lidar
Count
10000
100
1

```
##
## [[3]]
```

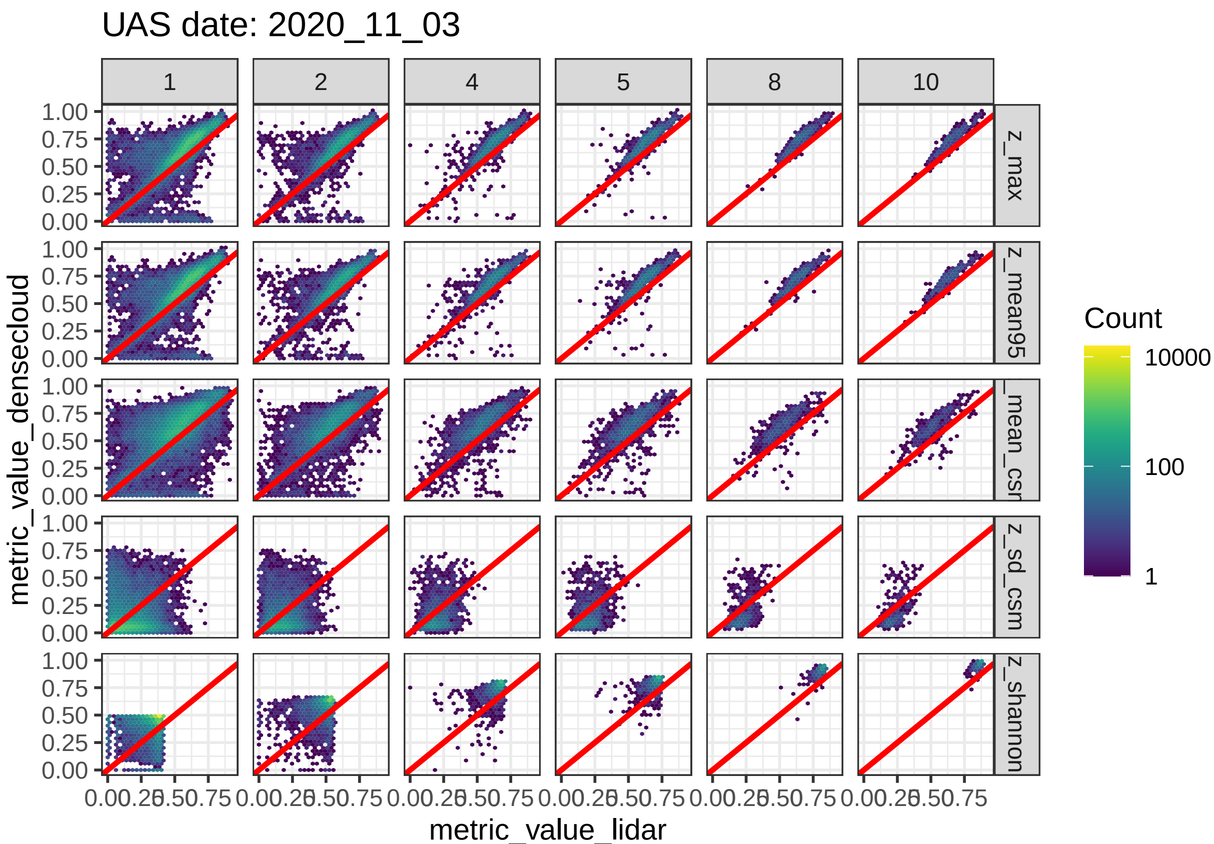

UAS date: 2020_11_03
1
2
4
5
8
10
z_max
z_mean95
_mean_csr
z_sd_csm
z_shannon
1.00
0.75
0.50
0.25
0.00
metric_value_densecloud
0.00.20.50.75
metric_value_lidar
Count
10000
100
1


```
##
## [[4]]
```

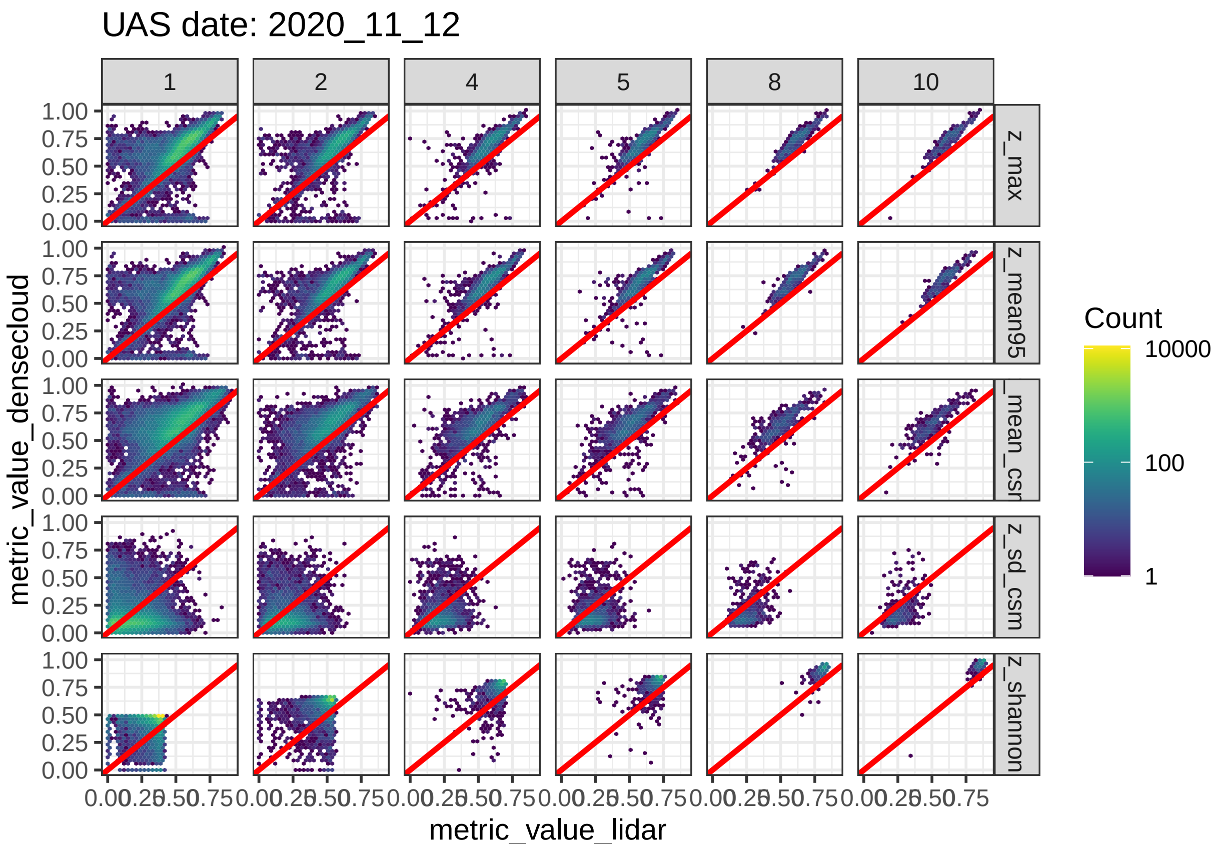

Date Summary

all these plots use a 2m resolution for the indice calculation

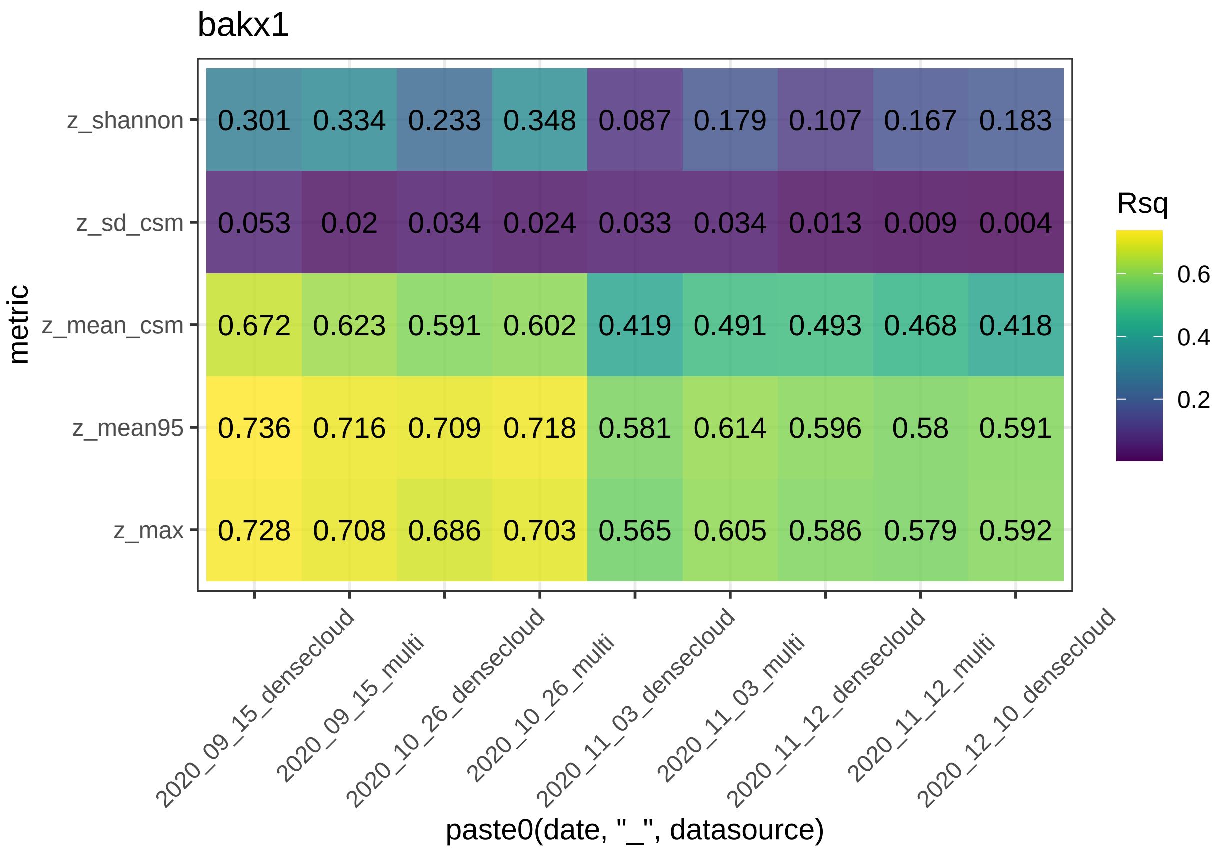
bakx1
metric
z_shannon
z_sd_csm
z_mean_csm
z_mean95
z_max
0.301 0.334 0.233 0.348 0.087 0.179 0.107 0.167 0.183
0.053 0.02 0.034 0.024 0.033 0.034 0.013 0.009 0.004
0.672 0.623 0.591 0.602 0.419 0.491 0.493 0.468 0.418
0.736 0.716 0.709 0.718 0.581 0.614 0.596 0.58 0.591
0.728 0.708 0.686 0.703 0.565 0.605 0.586 0.579 0.592
2020_09_15_densecloud
2020_09_15_multi
2020_10_26_densecloud
2020_10_26_multi
2020_11_03_densecloud
2020_11_03_multi
2020_11_12_densecloud
2020_11_12_multi
2020_12_10_densecloud
paste0(date, "_", datasource)
Rsq
0.6
0.4
0.2

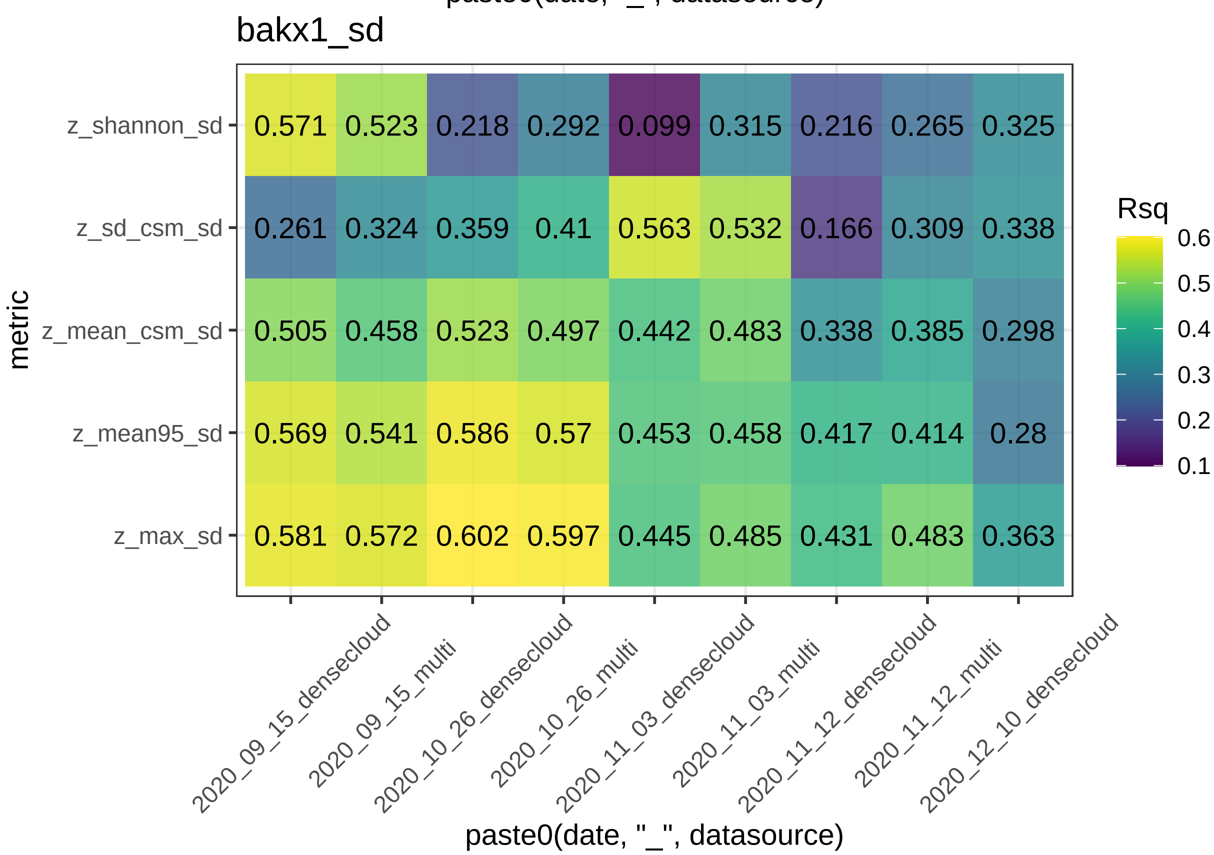
bakx1_sd
metric
z_shannon_sd
z_sd_csm_sd
z_mean_csm_sd
z_mean95_sd
z_max_sd
0.571 0.523 0.218 0.292 0.099 0.315 0.216 0.265 0.325
0.261 0.324 0.359 0.41 0.563 0.532 0.166 0.309 0.338
0.505 0.458 0.523 0.497 0.442 0.483 0.338 0.385 0.298
0.569 0.541 0.586 0.57 0.453 0.458 0.417 0.414 0.28
0.581 0.572 0.602 0.597 0.445 0.485 0.431 0.483 0.363
2020_09_15_densecloud
2020_09_15_multi
2020_10_26_densecloud
2020_10_26_multi
2020_11_03_densecloud
2020_11_03_multi
2020_11_12_densecloud
2020_11_12_multi
2020_12_10_densecloud
paste0(date, "_", datasource)
Rsq
0.6
0.5
0.4
0.3
0.2
0.1

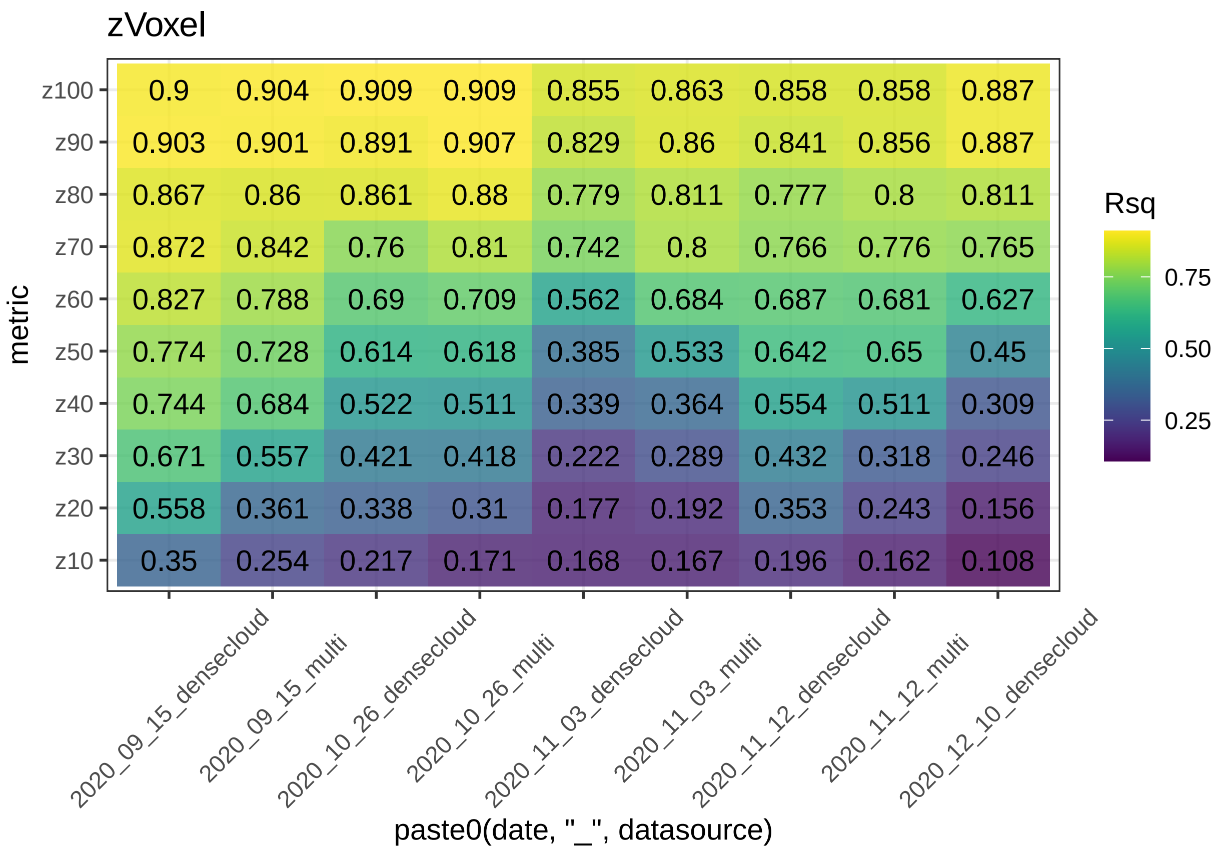
zVoxel
metric
z100
z90
z80
z70
z60
z50
z40
z30
z20
z10
0.9 0.904 0.909 0.909 0.855 0.863 0.858 0.858 0.887
0.903 0.901 0.891 0.907 0.829 0.86 0.841 0.856 0.887
0.867 0.86 0.861 0.88 0.779 0.811 0.777 0.8 0.811
0.872 0.842 0.76 0.81 0.742 0.8 0.766 0.776 0.765
0.827 0.788 0.69 0.709 0.562 0.684 0.687 0.681 0.627
0.774 0.728 0.614 0.618 0.385 0.533 0.642 0.65 0.45
0.744 0.684 0.522 0.511 0.339 0.364 0.554 0.511 0.309
0.671 0.557 0.421 0.418 0.222 0.289 0.432 0.318 0.246
0.558 0.361 0.338 0.31 0.177 0.192 0.353 0.243 0.156
0.35 0.254 0.217 0.171 0.168 0.167 0.196 0.162 0.108
2020_09_15_densecloud
2020_09_15_multi
2020_10_26_densecloud
2020_10_26_multi
2020_11_03_densecloud
2020_11_03_multi
2020_11_12_densecloud
2020_11_12_multi
2020_12_10_densecloud
paste0(date, "_", datasource)
Rsq
0.75
0.50
0.25

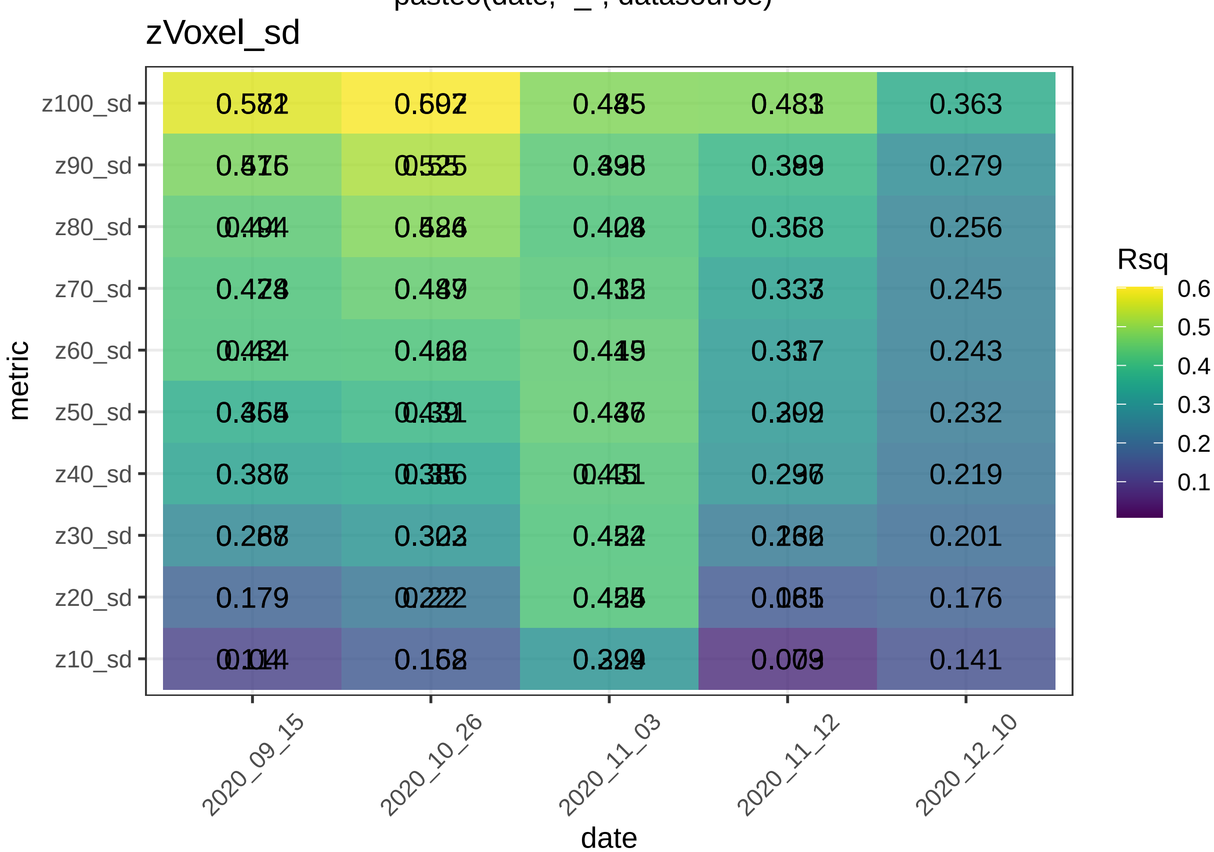
zVoxel_sd
metric
z100_sd
z90_sd
z80_sd
z70_sd
z60_sd
z50_sd
z40_sd
z30_sd
z20_sd
z10_sd
0.363
0.279
0.256
0.245
0.243
0.232
0.219
0.201
0.179
0.176
0.141
2020_09_15
2020_10_26
2020_11_03
2020_11_12
2020_12_10
date
Rsq
0.6
0.5
0.4
0.3
0.2
0.1

Discussion

Outlook: posibility of individual tree segmentation and then relate to stand variable (Sackov 2019) or even tree health (Belmonte 2018)

Bad correlations in lower voxel between LiDAR and UAS pointcloud might be because leaf off UAS is able to capture more branches and stems, therefore more points in lower part of the pointcloud (see Fig Distributions). UAS therefore might be better than LiDAR to capture understory vegetation (or at least the potential for understory vegetation) than leaf off LiDAR data The influence of understory to forest classifications is one common challenge in many studies and identified as a crucial week point

Text fragments

The main challange for further usage of Lidar data in a forest environment is the detection of individual trees. This enables the estimation of tree related parameters such as diameter at breast height, timber volume or crown related metrics (van Leeuwen and Nieuwenhuis 2010). Forest structure then can be described as the sum of the structure of individual trees (e.g. their height and biomass Ferraz et al. 2016) and the species composition (REF). This could give new insights into ecosystem functioning, since many processes and species distributions depend on functions provided by trees or their related microhabitats (REF). Further, monitoring of individual tree health and drought could be applied in forestry.

References

Alexander, Cici, Peder Klith Bøcher, Lars Arge, and Jens-Christian Svenning. 2014. "Regional-Scale Mapping of Tree Cover, Height and Main Phenological Tree Types Using Airborne Laser Scanning Data." *Remote Sensing of Environment* 147 (May): 156–72. https://doi.org/10.1016/j.rse.2014.02.013.

Bakx, Tristan R. M., Zsófia Koma, Arie C. Seijmonsbergen, and W. Daniel Kissling. 2019. "Use and Categorization of Light Detection and Ranging Vegetation Metrics in Avian Diversity and Species Distribution Research." Edited by Damaris Zurell. *Diversity and Distributions* 25 (7): 1045–59. https://doi.org/10.1111/ddi.12915.

Beland, Martin, Geoffrey Parker, Ben Sparrow, David Harding, Laura Chasmer, Stuart Phinn, Alexander Antonarakis, and Alan Strahler. 2019. "On Promoting the Use of Lidar Systems in Forest Ecosystem Research." *Forest Ecology and Management* 450 (October): 117484. https://doi.org/10.1016/j.foreco.2019.117484.

Cao, Lin, Hao Liu, Xiaoyao Fu, Zhengnan Zhang, Xin Shen, and Honghua Ruan. 2019. "Comparison of UAV LiDAR and Digital Aerial Photogrammetry Point Clouds for Estimating Forest Structural Attributes in Subtropical Planted Forests." *Forests* 10 (2): 145. https://doi.org/10.3390/f10020145.

Carrasco, Luis, Xingli Giam, Monica Papeş, and Kimberly Sheldon. 2019. "Metrics of Lidar-Derived 3d Vegetation Structure Reveal Contrasting Effects of Horizontal and Vertical Forest Heterogeneity on Bird Species Richness." *Remote Sensing* 11 (7): 743. https://doi.org/10.3390/rs11070743.

Davison, Sophie, Daniel N. M. Donoghue, and Nikolaos Galiatsatos. 2020. "The Effect of Leaf-on and Leaf-Off Forest Canopy Conditions on LiDAR Derived Estimations of Forest Structural Diversity." *International Journal of Applied Earth Observation and Geoinformation* 92 (October): 102160. https://doi.org/10.1016/j.jag.2020.102160.

Duncanson, Laura, and Ralph Dubayah. 2018. "Monitoring Individual Tree-Based Change with Airborne Lidar." *Ecology and Evolution* 8 (10): 5079–89. https://doi.org/10.1002/ece3.4075.

Fallati, Luca, Luca Saponari, Alessandra Savini, Fabio Marchese, Cesare Corselli, and Paolo Galli. 2020. "Multi-Temporal UAV Data and Object-Based Image Analysis (OBIA) for Estimation of Substrate Changes in a Post-Bleaching Scenario on a Maldivian Reef." *Remote Sensing* 12 (13): 2093. https://doi.org/10.3390/rs12132093.

Fawcett, Dominic, Benjamin Azlan, Timothy C. Hill, Lip Khoon Kho, Jon Bennie, and Karen Anderson. 2019. "Unmanned Aerial Vehicle (UAV) Derived Structure-from-Motion Photogrammetry Point Clouds for Oil Palm (*Elaeis Guineensis*) Canopy Segmentation and Height Estimation." *International Journal of Remote Sensing* 40 (19): 7538–60. https://doi.org/10.1080/01431161.2019.1591651.

Ferraz, António, Sassan Saatchi, Clément Mallet, and Victoria Meyer. 2016. "Lidar Detection of Individual Tree Size in Tropical Forests." *Remote Sensing of Environment* 183 (September): 318–33. https://doi.org/10.1016/j.rse.2016.05.028.

Froidevaux, Jérémy S. P., Florian Zellweger, Kurt Bollmann, Gareth Jones, and Martin K. Obrist. 2016. "From Field Surveys to LiDAR: Shining a Light on How Bats Respond to Forest Structure." *Remote Sensing of Environment* 175 (March): 242–50. https://doi.org/10.1016/j.rse.2015.12.038.

Ganz, Selina, Yannek Käber, and Petra Adler. 2019. "Measuring Tree Height with Remote Sensing—A Comparison of Photogrammetric and LiDAR Data with Different Field Measurements." *Forests* 10 (8): 694. https://doi.org/10.3390/f10080694.

Grüner, Esther, Thomas Astor, and Michael Wachendorf. 2019. "Biomass Prediction of Heterogeneous Temperate Grasslands Using an SfM Approach Based on UAV Imaging." *Agronomy* 9 (2): 54. https://doi.org/10.3390/agronomy9020054.

Guerra-Hernández, Juan, Eduardo González-Ferreiro, Vicente Monleón, Sonia Faias, Margarida Tomé, and Ramón Díaz-Varela. 2017. "Use of Multi-Temporal UAV-Derived Imagery for Estimating Individual Tree Growth in Pinus Pinea Stands." *Forests* 8 (8): 300. https://doi.org/10.3390/f8080300.

Hilmers, Torben, Nicolas Friess, Claus Bässler, Marco Heurich, Roland Brandl, Hans Pretzsch, Rupert Seidl, and Jörg Müller. 2018. "Biodiversity Along Temperate Forest Succession." Edited by Nathalie Butt. *Journal of Applied Ecology* 55 (6): 2756–66. https://doi.org/10.1111/1365-2664.13238.

Jeronimo, Sean M A, Van R Kane, Derek J Churchill, Robert J McGaughey, and Jerry F Franklin. 2018. "Applying LiDAR Individual Tree Detection to Management of Structurally Diverse Forest Landscapes." *Journal of Forestry* 116 (4): 336–46. https://doi.org/10.1093/jofore/fvy023.

Kamoske, Aaron G., Kyla M. Dahlin, Scott C. Stark, and Shawn P. Serbin. 2019. "Leaf Area Density from Airborne LiDAR: Comparing Sensors and Resolutions in a Temperate Broadleaf Forest Ecosystem." *Forest Ecology and Management* 433 (February): 364–75. https://doi.org/10.1016/j.foreco.2018.11.017.

Krause, Stuart, Tanja G. M. Sanders, Jan-Peter Mund, and Klaus Greve. 2019. "UAV-Based Photogrammetric Tree Height Measurement for Intensive Forest Monitoring." *Remote Sensing* 11 (7): 758. https://doi.org/10.3390/rs11070758.

Lee, Chung-Cheng, and Chi-Kuei Wang. 2018. "Estimating Stand Density in a Tropical Broadleaf Forest Using Airborne LiDAR Data." *Forests* 9 (8): 475. https://doi.org/10.3390/f9080475.

Lee, Junghee, Jungho Im, Kyungmin Kim, and Lindi Quackenbush. 2018. "Machine Learning Approaches for Estimating Forest Stand Height Using Plot-Based Observations and Airborne LiDAR Data." *Forests* 9 (5): 268. https://doi.org/10.3390/f9050268.

Ludwig, Marvin, Christian M. Runge, Nicolas Friess, Tiziana L. Koch, Sebastian Richter, Simon Seyfried, Luise Wraase, et al. 2020. "Quality Assessment of Photogrammetric Methods—A Workflow for Reproducible UAS Orthomosaics." *Remote Sensing* 12 (22): 3831. https://doi.org/10.3390/rs12223831.

Madsen, Bjarke, Urs A. Treier, András Zlinszky, Arko Lucieer, and Signe Normand. 2020. "Detecting Shrub Encroachment in Seminatural Grasslands Using UAS LiDAR." *Ecology and Evolution* 10 (11): 4876–4902. https://doi.org/10.1002/ece3.6240.

Malambo, L., S. C. Popescu, S. C. Murray, E. Putman, N. A. Pugh, D. W. Horne, G. Richardson, et al. 2018. "Multitemporal Field-Based Plant Height Estimation Using 3d Point Clouds Generated from Small Unmanned Aerial Systems High-Resolution Imagery." *International Journal of Applied Earth Observation and Geoinformation* 64 (February): 31–42. https://doi.org/10.1016/j.jag.2017.08.014.

Manfreda, Salvatore, Matthew F McCabe, Pauline E Miller, Richard Lucas, Victor Pajuelo Madrigal, Giorgos Mallinis, Eyal Ben Dor, et al. 2018. "On the Use of Unmanned Aerial Systems for Environmental Monitoring," 28.

Melin, M., J. Matala, L. Mehtätalo, J. Pusenius, and P. Packalen. 2016. "Ecological Dimensions of Airborne Laser Scanning — Analyzing the Role of Forest Structure in Moose Habitat Use Within a Year." *Remote Sensing of Environment* 173 (February): 238–47. https://doi.org/10.1016/j.rse.2015.07.025.

Michez, Adrien, Leo Huylenbroeck, Corentin Bolyn, Nicolas Latte, Sébastien Bauwens, and Philippe Lejeune. 2020. "Can Regional Aerial Images from Orthophoto Surveys Produce High Quality Photogrammetric Canopy Height Model? A Single Tree Approach in Western Europe." *International Journal of Applied Earth Observation and Geoinformation* 92 (October): 102190. https://doi.org/10.1016/j.jag.2020.102190.

Moeckel, Thomas, Supriya Dayananda, Rama Nidamanuri, Sunil Nautiyal, Nagaraju Hanumaiah, Andreas Buerkert, and Michael Wachendorf. 2018. "Estimation of Vegetable Crop Parameter by Multi-Temporal UAV-Borne Images." *Remote Sensing* 10 (5): 805. https://doi.org/10.3390/rs10050805.

Montgomery, Joshua, Brian Brisco, Laura Chasmer, Kevin Devito, Danielle Cobbaert, and Chris Hopkinson. 2019. "SAR and Lidar Temporal Data Fusion Approaches to Boreal Wetland Ecosystem Monitoring." *Remote Sensing* 11 (2): 161. https://doi.org/10.3390/rs11020161.

Ota, Tetsuji, Miyuki Ogawa, Katsuto Shimizu, Tsuyoshi Kajisa, Nobuya Mizoue, Shigejiro Yoshida, Gen Takao, et al. 2015. "Aboveground Biomass Estimation Using Structure from Motion Approach with Aerial Photographs in a Seasonal Tropical Forest." *Forests* 6 (12): 3882–98. https://doi.org/10.3390/f6113882.

Roussel, Jean-Romain, David Auty, Nicholas C. Coops, Piotr Tompalski, Tristan R. H. Goodbody, Andrew Sánchez Meador, Jean-François Bourdon, Florian de Boissieu, and Alexis Achim. 2020. "lidR: An R Package for Analysis of Airborne Laser Scanning (ALS) Data." *Remote Sensing of Environment* 251 (December): 112061. https://doi.org/10.1016/j.rse.2020.112061.

Shi, Yifang, Tiejun Wang, Andrew K. Skidmore, and Marco Heurich. 2018. "Important LiDAR Metrics for Discriminating Forest Tree Species in Central Europe." *ISPRS Journal of Photogrammetry and Remote Sensing* 137 (March): 163–74. https://doi.org/10.1016/j.isprsjprs.2018.02.002.

Silva, Carlos A., Andrew T. Hudak, Lee A. Vierling, E. Louise Loudermilk, Joseph J. O'Brien, J. Kevin Hiers, Steve B. Jack, et al. 2016. "Imputation of Individual Longleaf Pine (*Pinus Palustris* Mill.) Tree Attributes from Field and LiDAR Data." *Canadian Journal of Remote Sensing* 42 (5): 554–73. https://doi.org/10.1080/07038992.2016.1196582.

Simonson, William D., Harriet D. Allen, and David A. Coomes. 2014. "Applications of Airborne Lidar for the Assessment of Animal Species Diversity." Edited by Andrew Tatem. *Methods in Ecology and Evolution* 5 (8): 719–29. https://doi.org/10.1111/2041-210X.12219.

Ullah, Sami, Matthias Dees, Pawan Datta, Petra Adler, Mathias Schardt, and Barbara Koch. 2019. "Potential of Modern Photogrammetry Versus Airborne Laser Scanning for Estimating Forest Variables in a Mountain Environment." *Remote Sensing* 11 (6): 661. https://doi.org/10.3390/rs11060661.

Valbuena, R., B. O'Connor, F. Zellweger, W. Simonson, P. Vihervaara, M. Maltamo, C. A. Silva, et al. 2020. "Standardizing Ecosystem Morphological Traits from 3d Information Sources." *Trends in Ecology & Evolution* 35 (8): 656–67. https://doi.org/10.1016/j.tree.2020.03.006.

van Iersel, Wimala, Menno Straatsma, Hans Middelkoop, and Elisabeth Addink. 2018. "Multitemporal Classification of River Floodplain Vegetation Using Time Series of UAV Images." *Remote Sensing* 10 (7): 1144. https://doi.org/10.3390/rs10071144.

van Leeuwen, Martin, and Maarten Nieuwenhuis. 2010. "Retrieval of Forest Structural Parameters Using LiDAR Remote Sensing." *European Journal of Forest Research* 129 (4): 749–70. https://doi.org/10.1007/s10342-010-0381-4.

Xu, Zhong, Xin Shen, Lin Cao, Nicholas C. Coops, Tristan R. H. Goodbody, Tai Zhong, Weidong Zhao, et al. 2020. "Tree Species Classification Using UAS-Based Digital Aerial Photogrammetry Point Clouds and Multispectral Imageries in Subtropical Natural Forests.” *International Journal of Applied Earth Observation and Geoinformation* 92 (October): 102173. https://doi.org/10.1016/j.jag.2020.102173.

Ye, Ning, Louise van Leeuwen, and Panagiotis Nyktas. 2019. “Analysing the Potential of UAV Point Cloud as Input in Quantitative Structure Modelling for Assessment of Woody Biomass of Single Trees.” *International Journal of Applied Earth Observation and Geoinformation* 81 (September): 47–57. https://doi.org/10.1016/j.jag.2019.05.010.